Applied Catalysis A: General 403 (2011) 91–97

Contents lists available at ScienceDirect

Applied Catalysis A: General

journal homepage: www.elsevier.com/locate/apcata

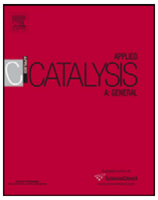

In situ encapsulation of Pt nanoparticles in mesoporous silica: Synthesis, characterisation and effect of particle size on CO oxidation

Atul K. Prashar[a], S. Mayadevi[b], P.R. Rajamohanan[c], R. Nandini Devi[a,*]

[a] Catalysis and Inorganic Chemistry Division, National Chemical Laboratory, Dr. Homi Bhabha Road, Pune 411008, India
[b] Chemical Engineering and Process Development Division, National Chemical Laboratory, Dr. Homi Bhabha Road, Pune 411008, India
[c] Central NMR Facility, National Chemical Laboratory, Dr. Homi Bhabha Road, Pune 411008, India

ARTICLE INFO

Article history:
Received 11 April 2011
Received in revised form 13 June 2011
Accepted 16 June 2011
Available online 23 June 2011

Keywords:
In situ synthesis
Pt nanoparticle
Mesoporous silica
CO oxidation

ABSTRACT

Pt nanoparticles of narrow size distribution and average particle size of 4.4 nm are isolated exclusively inside SBA-12 mesoporous silica by a novel in situ method. The interaction of Pt precursor with surfactant–polymer composite micelle is followed by NMR and UV studies. The final Pt incorporated silica material is characterised by XRD, TEM and N_2 adsorption. The mesoporous nature of the silica is found to be intact after Pt incorporation without any pore blockage. CO oxidation activity of this material is compared with that of mesoporous silica incorporating different sizes of Pt viz., 1.8, 3.6 and 8 nm. Activation energies of CO oxidation for all these materials are calculated by a simple differential method based on first principles. A comparison of activation energies and single site yields reveals that these parameters are distinguishably less in catalyst containing 1.8 nm Pt nanoparticles but more or less same in catalysts containing 3.6, 4.4 and 8 nm Pt nanoparticles.

1. Introduction

Noble metal nanoparticles have found application in various fields recently including medicine, optics and electronics [1–5]. However, peculiar surface structure of fine particles and their importance has been known to catalysis community for nearly a century [6]. Even though major advances have been achieved in nanoparticle synthesis [7–13] controlling and fine tuning their size and shape is still a challenging feat. This is particularly true in case of supported catalyst materials, wherein conventional methods are fraught with poor size distribution and tendency for sintering at higher temperatures. Fortunately, utilization of mesoporous compounds as supports opens a new avenue for addressing these problems, whereby sintering can be minimised by isolating the nanoparticles inside the channels or cavities [14–16]. However, special steps need to be taken to prevent nanoparticles depositing on the outside surface of the channels leading to agglomeration. In this context, we have developed a simple method for in situ synthesis of nanoparticles as well as encapsulating them exclusively within the channels of mesoporous silica.

Our strategy was to add controlled amounts of an ionic surfactant to the templating nonionic polymer so that a composite is formed in which the ionic head groups of the surfactant molecules are dispersed in the corona of the polymer micelle. In this way, the metal precursors could be anchored by electrostatic attraction to the ionic head groups and when silica wall formed around the template, they were present exclusively within the channels formed by the template. We have successfully used this method for synthesising monodisperse ~8 nm spherical particles by employing cetyltrimethylammonium bromide (CTAB)–polyethylene polypropylene block copolymer (P123) composite as template for the preparation of SBA-15 [17]. In this strategy, silica walls delimit the growth of the nanoparticles and the channels act as moulds for shaping them. Hence polymer–surfactant composite micelles of various sizes can be utilized for anchoring metal precursors. These composites with anchored metal precursors, while acting as templates for the growth of silica, ensure the presence of metal nanoparticles within the channels on subsequent calcination and removal of organics. In the present work, we have selected the composite micelle system of Brij 76 [$(CH_3(CH_2)_{17}(EO)_{10}$] and CTAB for anchoring the metal precursor. The polymer Brij 76 is known to template the formation of SBA-12 [18,19] type of mesoporous silica compounds with channel size of ~5 nm. Dispersion of H_2PtCl_6 in Brij 76–CTAB composite and synthesis of mesoporous silica using this template and further calcination has led to the formation of spheroid Pt nanoparticles with average size of 4.4 nm.

In the recent past, studies have shown the importance of size and shape of nanoparticles in catalysis, especially in the range of 1–10 nm [20–27]. This effect is believed to be due to the changes in electronic and attendant surface structure variations with changes in particle size. When the particles are very small, i.e. subnanome-

---

* Corresponding author. Tel.: +91 20 25902271; fax: +91 20 25902063.
E-mail address: nr.devi@ncl.res.in (R. Nandini Devi).

0926-860X/$ – see front matter © 2011 Elsevier B.V. All rights reserved.
doi:10.1016/j.apcata.2011.06.016

ter to ~2 nm, consisting of only a few to tens of atoms, quantum confinement effects set in with molecule-like orbital characteristics. In bigger particles with sizes >2 nm, surface plasmon resonance evolves. Such electronic characteristics render these materials with unique surface properties ideal for catalysis [28,29]. We have studied this effect by comparing the kinetics and activation energy of CO oxidation in Pt nanoparticles of average sizes 1.8, 3.6, 4.4 and 8 nm encapsulated in mesoporous silica materials. It is found that single site yield and activation energies are distinguishably more in 1.8 nm particles when compared to 3.6, 4.4 and 8 nm particles which show more or less same values.

2. Experimental

2.1. Synthesis of SBA-12 mesoporous silica

SBA-12 was prepared using Brij 76–CTAB composite with varying concentrations of CTAB in a fixed amount of Brj 76 (4 wt%). Typically, CTAB (Aldrich) was added to 50 g of 4 wt% solution of nonionic surfactant Brij 76 (Aldrich, $C_{18}EO_{10}$) and this mixture was stirred for 24 h at 308–313 K and kept overnight for stabilisation at room temperature. This solution was made acidic (pH < 2) by adding 3 g of conc. HCl (37%). After 3 h, 4.25 g of tetraethylorthosilicate (TEOS; Aldrich) was added under stirring. Stirring was continued for another 24 h at 313 K and then autoclaved at 373 K for 48 h. The solid product was filtered, washed, dried and calcined at 773 K for 12 h for enabling the template removal. The CTAB concentration was progressively increased to 64 mM in 4 wt% Brij 76 for different samples. The final molar composition of the gel was 1 TEOS:0.13 Brij 76:1.5 HCl:139 H_2O:0–0.16 CTAB.

2.2. Synthesis of Pt/SBA-12

Typically, CTAB was added to 50 g of 4 wt% solution of nonionic surfactant Brij 76 so that the final concentration was 2 mM of CTAB and this mixture was stirred for 24 h at 308–313 K and kept overnight for stabilisation at room temperature. For Pt incorporation, 2.6 mL of 0.019 M solution of $H_2PtCl_6 \cdot 6H_2O$ (Aldrich) was added to the Brij 76–CTAB composite solution and stirred for 24 h at 313 K. This solution was made acidic (pH < 2) by adding 3 g of conc. HCl (37%). After 3 h, 4.25 g of tetraethylorthosilicate (TEOS; Aldrich) was added under stirring. Stirring was continued for another 24 h at 313 K and then whole gel was autoclaved at 373 K for 48 h. The solid product was filtered, washed, dried and calcined at 773 K for 12 h for enabling the template removal. The final molar composition of the gel was 1 TEOS:139 H_2O:1.5 HCl:0.13 Brij 76:0.005 CTAB:0.0025 $H_2PtCl_6 \cdot 6H_2O$.

2.3. Synthesis of Pt/SBA15

Pt particles with average sizes of 1.8 and 3.6 nm were synthesised by alcohol reduction method and incorporated in the channels of mesoporous SBA-15 by sonication as reported elsewhere [30]. In situ method as reported by us [17] was followed for the synthesis of Pt with average size of 8 nm encapsulated in SBA-15.

2.4. Characterisation

All the NMR measurements were carried out on a Bruker AV400 NMR spectrometer operating at 400 MHz for ^1H using a standard 5 mm BBFO probe. The sample solutions were prepared by dissolving the required amount of sample in 99.98% D_2O and the measurements were performed at room temperature (23 °C) and 40 °C using internal reference of 3-trimethylsilyl propionic acid 2,2,3,3, d_4 sodium salt (TSP d_4) at 0 ppm. UV–vis spectra were acquired using a Perkin Elmer Lambda 650 spectrometer. Ionic strengths of the solutions were normalized using KBr and the experiments were carried out in 1 mm quartz cuvettes. Powder X-ray diffraction of all the samples were carried out in a PANalytical X'pert Pro duel goniometer diffractometer. A proportional counter detector was used for low angle experiments and an X'celerator solid state detector was employed in wide angle experiments. The radiation used was Cu $K\alpha$ (1.5418 Å) with a Ni filter and the data collection was carried out using a flat holder in Bragg-Brentano geometry (0.2°/min). Care was taken to avoid sample displacement effects. HRTEM analysis was done with Tecnai (Model F30) operating at 300 kV. Samples were crushed and dispersed in isopropanol (IPA) with low power sonication before putting a drop over carbon coated Cu grid for observation. Particle size distribution was statistically analysed from TEM images using the program Digital Micrograph.

Nitrogen adsorption/desorption isotherms were acquired using Autosorb 1C Quantachrome USA. The program consisted of both adsorption and desorption branch and typically ran at −196 °C after samples were degassed at 250 °C for 2 h once the final temperature had been maintained. Specific surface areas were calculated via the BET model at relative pressures of $P/P_o = 0.06 - 0.3$. The total pore volume was estimated from the uptake of adsorbate at a relative pressure of $P/P_o = 0.99$. Pore size distribution curves were obtained via the NLDFT model assuming cylindrical pore geometry and the micropore volume calculated via *t*-plot analyses as a function of relative pressure using the Broekhoff de Boer model for thickness curve measured between 3.5 and 5.0 Å.

Chemical analysis was carried out in a Spectro Arcos ICP-OES instrument. Standard solutions were used for calibration purpose.

2.5. Catalyst evaluation

Catalytic runs were carried out in a fixed bed down flow glass reactor of diameter 14 mm at atmospheric pressure. Reactor gas flow from respective cylinders was controlled using mass flow controllers (Brooks) one each for N_2, O_2 and CO. The reactor was placed in a tubular furnace with a uniform heating zone of 4 cm and temperature of the furnace was controlled using Radix 6400 temperature controller. Catalyst bed temperature was measured using K-type thermocouple placed in a thermowell over the catalyst. The reactor outflow was analysed using a gas chromatograph equipped with online gas sampling valve, 91.44 cm molecular sieve 13X column and thermal conductivity detector (TCD). All the catalytic reactions were done in the temperature range of 433–571 K. Reactant gas mixture consisted of $9.55 \pm 0.55\%$ (v/v) CO, $6.13 \pm 0.37\%$ (v/v) O_2 and $84.3 \pm 1.3\%$ (v/v) N_2. Five different total flow rates, i.e. 20 ± 2, 40 ± 1, 60 ± 2, 80 ± 1.5 and $100 \pm 1\ cm^3\ min^{-1}$ of reactant gas mixture corresponding to GHSV values of 3000(±300), 6000(±150), 9000(±300), 12,000(±225) and 15,000(±150) $cm^3\ h^{-1}\ g_{cat}{}^{-1}$ respectively were used for each catalyst. Four different catalysts, i.e. Pt/SBA-15 (8 nm), Pt/SBA-12 (4.4 nm), Pt/SBA-15 (1.8 nm) and Pt/SBA-15 (3.6 nm) were studied. Although, originally all the catalysts contained different loadings of Pt, for the sake of comparison, Pt loading in each catalyst was made same (0.4 wt%) by diluting the catalyst with calcined SBA-15. 0.4 g of catalyst, pelletized and sieved through 0.5 mm sieves was loaded in the reactor. Prior to the reaction, each catalyst was activated/reduced at 673 K for 2 h with 2 K/min ramp rate under H_2 flow. Then temperature was lowered to 373 K and kept at that temperature for 1 h under N_2 flow ($10\ cm^3\ min^{-1}$). Subsequently the bed temperature was increased to 433 K and tested for its activity at this temperature. The bed temperature was increased in 10 K increments until the temperature of light off was reached and the steady state activity (outlet CO concentration) at each temperature was noted. For each reaction temperature, the reaction mixture was analysed after 30 min on stream for attaining steady state con-